Facilities and experimental techniques: reactions (neutron beams, reactors)

Arnd Junghans
Helmholtz-Zentrum Dresden-Rossendorf Germany

Table of Content

- Neutron production: quasimonoenergetic and white neutron beams (photonuclear, nuclear reactions, spallation, fission).
- Continuous and pulsed neutron beams (TOF)
- Neutron sources worldwide and in Europe
- Neutron sources for fission, capture, inelastic reactions and transmission experiments.

Neutron sources in nature

- Neutron sources in nature:
  Neutrons can be formed in nuclear reactions of high-energetic cosmic particles in the upper atmosphere. The flux is inversely proportional to the solar activity
  (high solar activity deformes the earth‘s magnetic field)
  and strongly dependend on the geographical latitude and altitude.

Gordon et. al. IEEE TNS 51 (2006) 3427

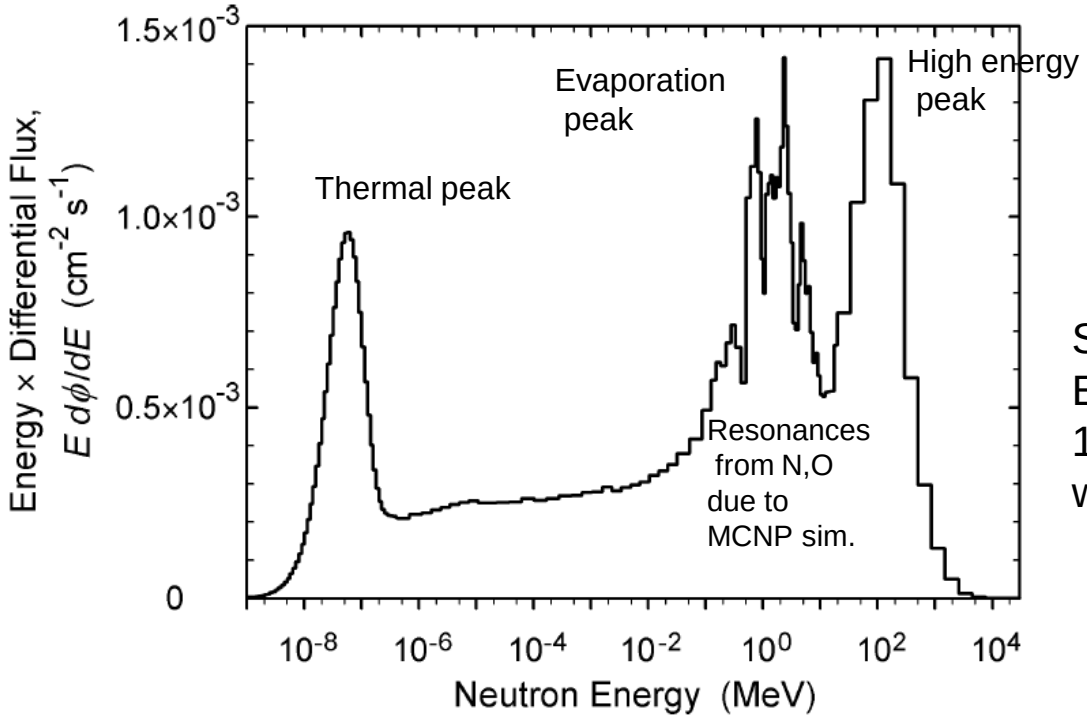

Fig. 4. Neutron spectrum measured on the roof of the IBM T. J. Watson Research Center in Yorktown Heights, NY.

Setup:
Extended range Bonner spheres
14 different size PE moderators
with ^{3}He proportional counters

G. Heusser, Low-radioactivity background techniques

Neutron producing nuclear reactions

- In two-body reactions monoenergetic neutrons can be produced, e.g. DT-reaction: T(D,n)^{4}He, Q = 17.16 MeV, D= ^{2}H, T=^{3}H
- Kinematics determines the angular distribution and energy spectrum
- The yield (neutrons /primary particles) is determined by the differential cross section $\frac{d\sigma}{d\Omega}(E_{pro}, \Theta)$
- Realistic yield determination by integration over the target thickness and angular range (slowing down of the beam in the target material)

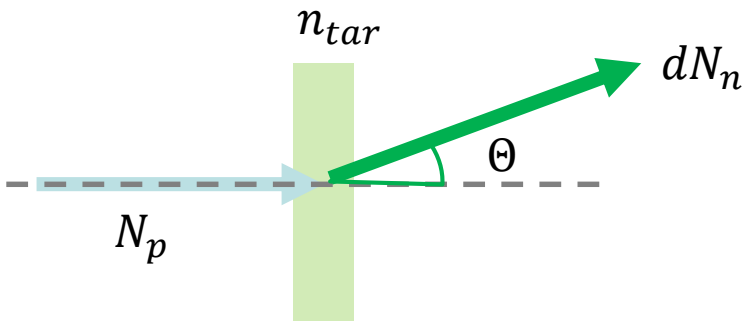

Important reactions for neutron production

	$D(d,n)^3He$	$T(p,n)^3He$	$T(d,n)^4He$	$^7Li(p,n)^7Be$
Q-value(MeV)	3.2689	-0.7638	17.589	-1.6442

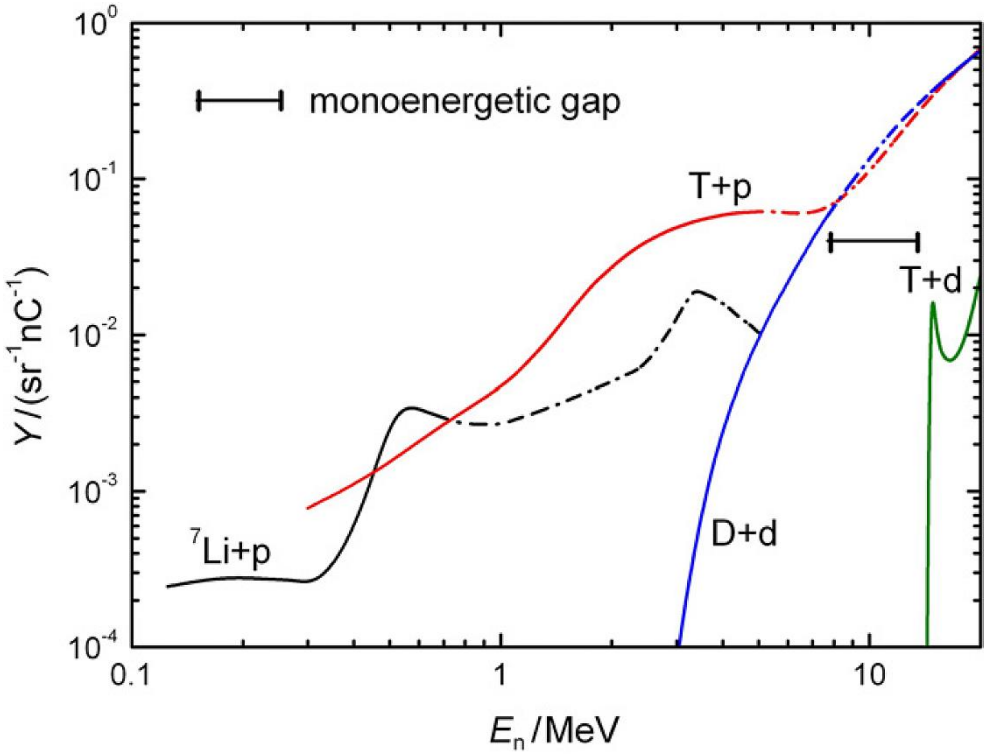

Neutron emission yield at 0°
With $\frac{\Delta E_n}{E_n} = 1\%$

quasimonoenergetic range indicated by dashed lines
breakup T(p,n), D(d,n)
^{7}Li(p,n)^{7}Be*

No monoenergetic neutrons in the Gap between 7.7 – 13.2 MeV

R. Nolte, D.J. Thomas, Metrologia 48 (2011) S263

Monoenergetic neutron reference fields

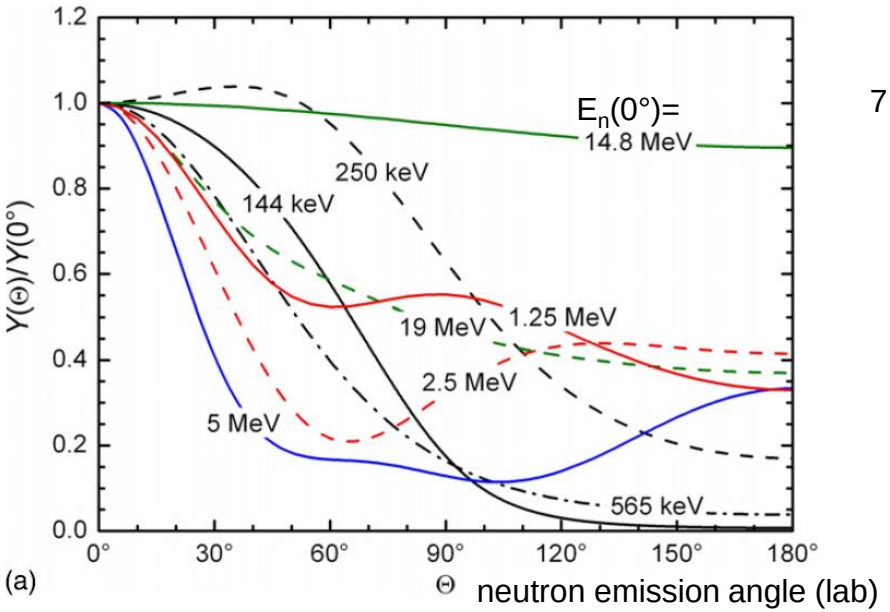

(a)

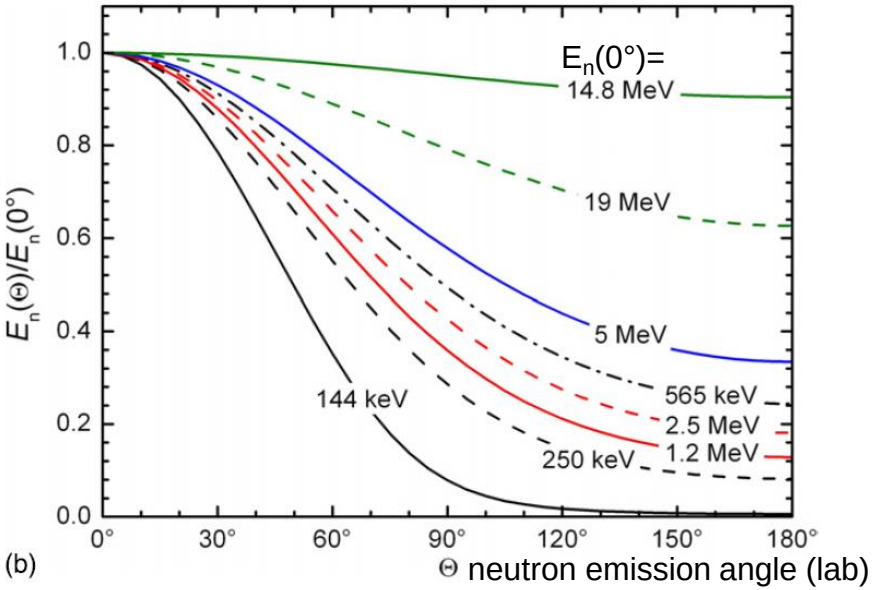

(b)

T(d,n)^{4}He
^{7}Li(p,n)^{7}Be
T(p,n)^{3}He
D(d,n)^{3}He

relative Yield
Y(0°) calculated for $\Delta E_n = 10$ keV

T(d,n)^{4}He:
rather isotropic

^{7}Li(p,n)^{7}Be:
production of keV neutrons at backward angles (reduced yield)

Parameters of reference fields
(E_n,Y, target, beam properties)
see table 2 of
R. Nolte, D.J. Thomas, Metrologia 48 (2011) S263

DROSG 2000 neutron source reactions code:
https://www-nds.iaea.org/public/libraries/drosg2000/

Relativistic two body kinematics:

- Lorentz-Transformation in beam direction with rapidity $Y = \ln \frac{p_{cm} + \sqrt{m_1^2 + p_{cm}^2}}{m_1}$

...

$$p_{3,4} = \frac{\sqrt{m_{3,4}^2 + p'^2_{cm}}\ \cos\Theta_{3,4} \sinh Y \pm \cosh Y \sqrt{p'^2_{cm} - m_{3,4}^2 \sin^2\Theta_{3,4} \sinh^2 Y}}{1 + \sin^2\Theta_{3,4} \sinh^2 Y}$$

- Two solutions of $p_{3,4} = f(\Theta_{3,4})$!
- For endothermic reactions $Q = m_1 + m_2 - m_3 - m_4 < 0$ MeV
  Forward threshold (minimum kinetic energy for the reaction to occur) derived from $E_{3,cm} + E_{4,cm} \geq \mathrm{m}_3 + \mathrm{m}_4$

$$T_f = -Q\left[1 + \left(\frac{m_2}{m_1}\right) - \left(\frac{Q}{2m_1}\right)\right]$$

- If the ejectile is slower than the c.m. velocity E_3 is a double-valued function of the lab angle Θ_3 . Equivalent: Θ_3 is a double-valued function of Θ_{cm} up to the back threshold $T_b = -Q\left[1 + \frac{m_2}{m_1 - m_3} - \frac{Q}{2(m_1 - m_3)}\right]$

Energy range for neutron production

- „Monoenergetic“ neutrons from reactions with only one neutron group
- „Quasi-monoenergetic“ neutrons from reactions with a second group of neutrons from reactions to excited states of the recoil or nuclear break up
- Example: $^{7}Li(p,n)^{7}Be$

Reaction	$^{7}Be^{*}$ Exc. Energy (MeV)	Q-value (MeV)	Threshold (MeV)
$^{7}Li(p,n)^{7}Be$	0	-1.644	1.881 forward 1.920 backward
$^{7}Li(p,n)^{7}Be^{*}$	0.429	-2.073	2.371 forward 2.421 backward
$^{7}Li(p,n^{3}He)^{4}He$	break-up	-3.229	3.692
$^{7}Li(p,n)^{7}Be^{**}$	4.57	-6.214	-7.110 forward -7.260 backward

- Energy levels of light nuclei, see http://www.tunl.duke.edu/nucldata/index.shtml

- Monoenergetic neutrons from E_p =1.920 MeV – 2.371 MeV
  E_n = 121 keV – 649 keV

^{7}Li(p,n)^{7}Be : neutron energy vs. angle

- Q=−1.644 MeV ; T_f = 1.881 MeV ; T_b = 1.920 MeV

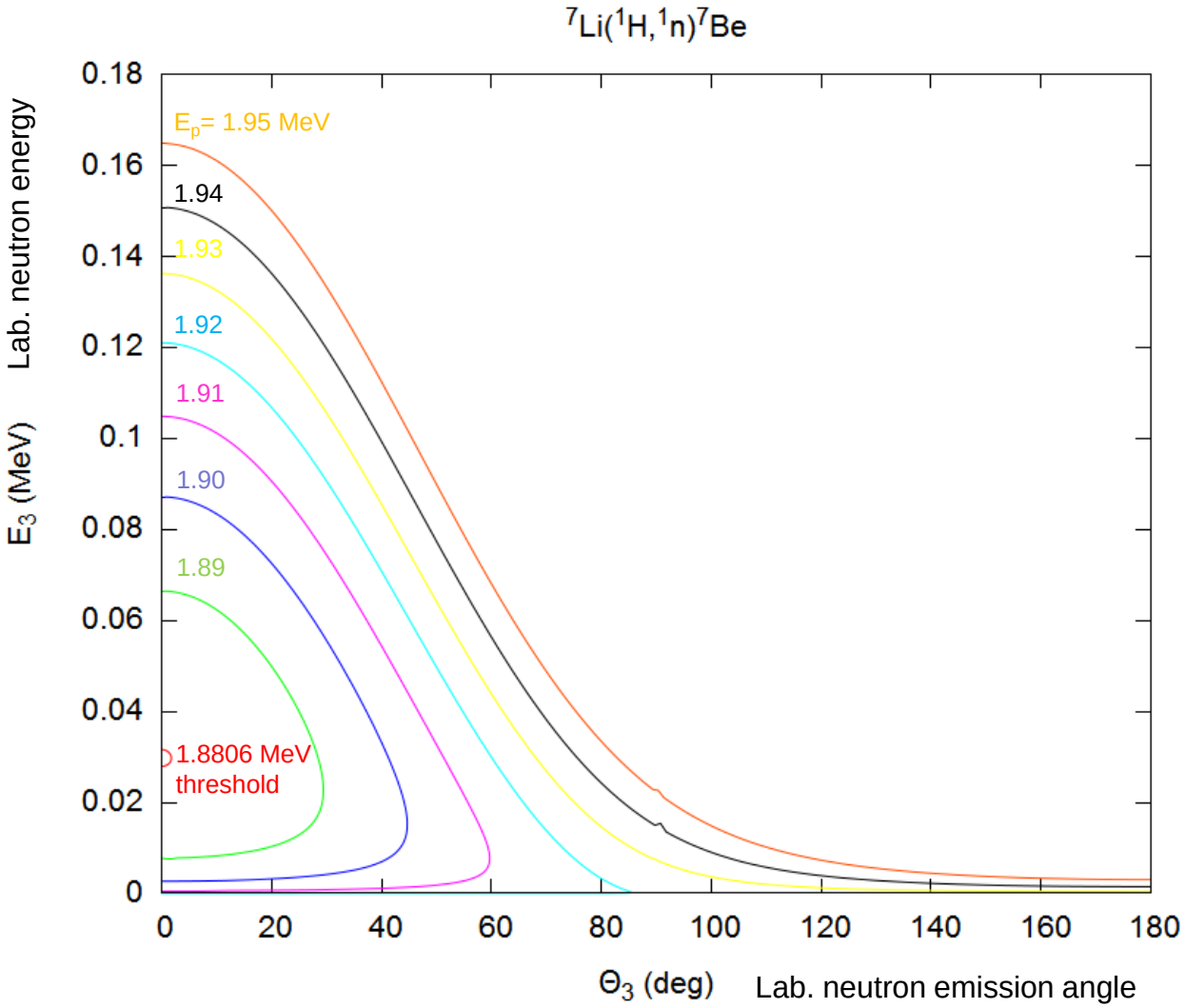

Two neutron energy groups below T_b

Neutron production in inverse kinematics

- light-ion beam required with higher energy (beam heating) e.g. $^{1}H(^{7}Li,n)^{7}Be$

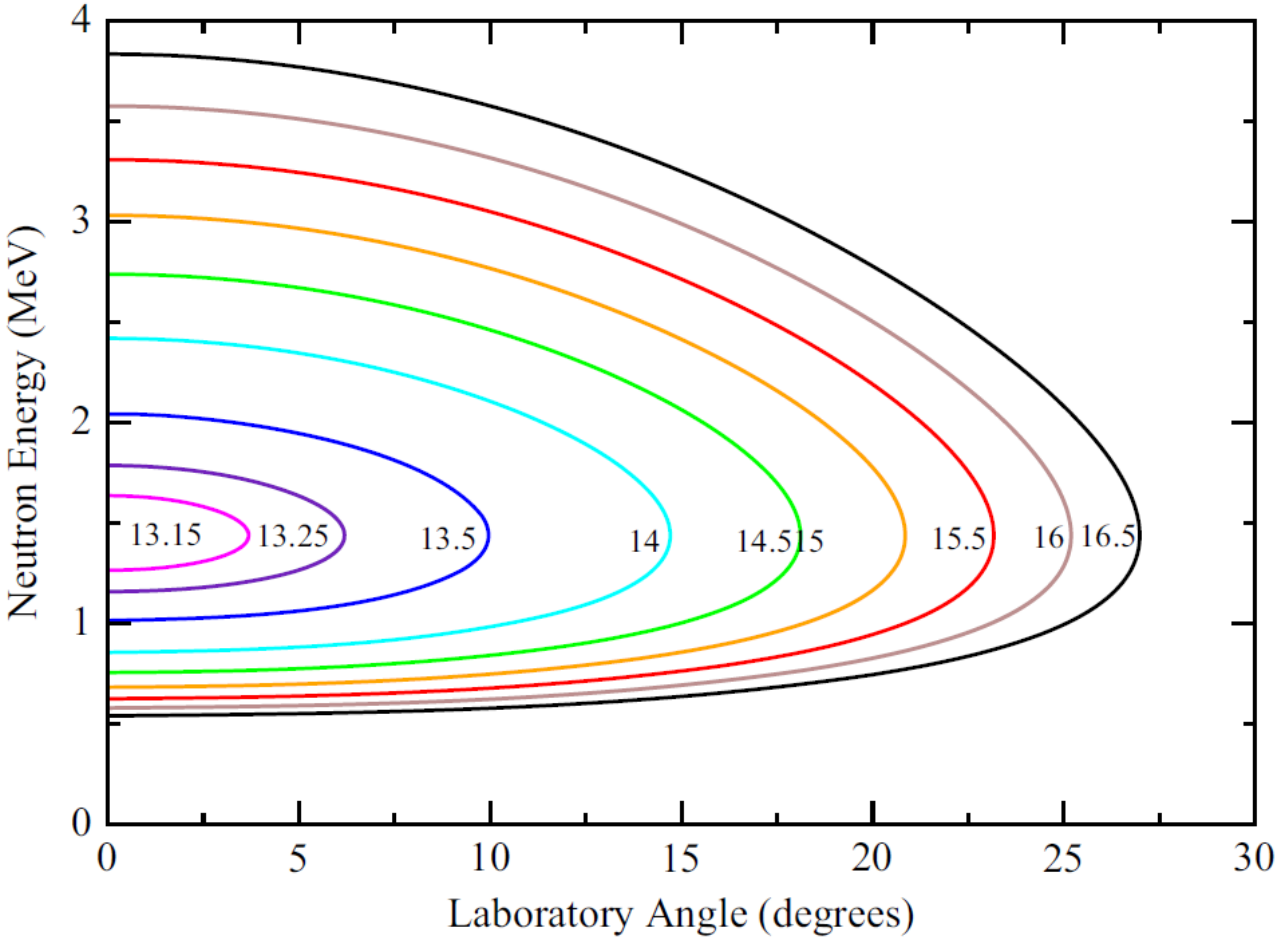

Kinematical focussing increases neutron intensity in a forward cone.
Licorne Facility at IPNO

$T_f = 13.096$ MeV

M. Lebois et al. NIM A735(2014)145–151

Fig. 1. Kinematic curves relating the angle of neutron emission to neutron energy in the laboratory frame for different ^{7}Li bombarding energies from 13.15 to 16.5 MeV, calculated using two-body relativistic kinematics.

Realistic source yield

The differential neutron spectrum

$$\frac{d^2N}{dE_n d\Omega} = N_p n_{tar} \left(\frac{d\sigma}{d\Omega^{cm}}\right)\left(\frac{d\Omega^{cm}}{d\Omega}\right)\left(\frac{\mathrm{dE_p}}{\mathrm{dx}}\right)^{-1}\left(\frac{\mathrm{dE_p}}{\mathrm{dE_n}}\right)$$

$$\mathrm{Y} = \int \frac{d^2N}{dE_n d\Omega}\frac{1}{N_p} dE_n$$

$\frac{\mathrm{dE_p}}{\mathrm{dx}}$ linear stopping power,
$\frac{d\Omega^{cm}}{d\Omega}$ solid angle element ratio c.m to laboratory system,
$\frac{\mathrm{dE_p}}{\mathrm{dE_n}}$ kinematic factor

- Neutron yield depends on target thickness and purity:
  Energy loss of the beam in the neutron producing target layer
  ➔ beam heating of the target
  Thermal motion of target atoms e.g. in gaseous targets
  ➔ neutron energy spread
- Neutron scattering in target materials, backings, windows
- Opening angle and source and detector counting geometry
- Kinematic focussing for reactions in inverse kinematics

➔ Monte Carlo neutron transport simulation to describe the neutron spectrum of quasimonoenergetic neutron sources

Time correlated associated particle method

➔ neutron yield measured independent from $\frac{d\sigma}{d\Omega^{cm}}$

PTB neutron reference facility

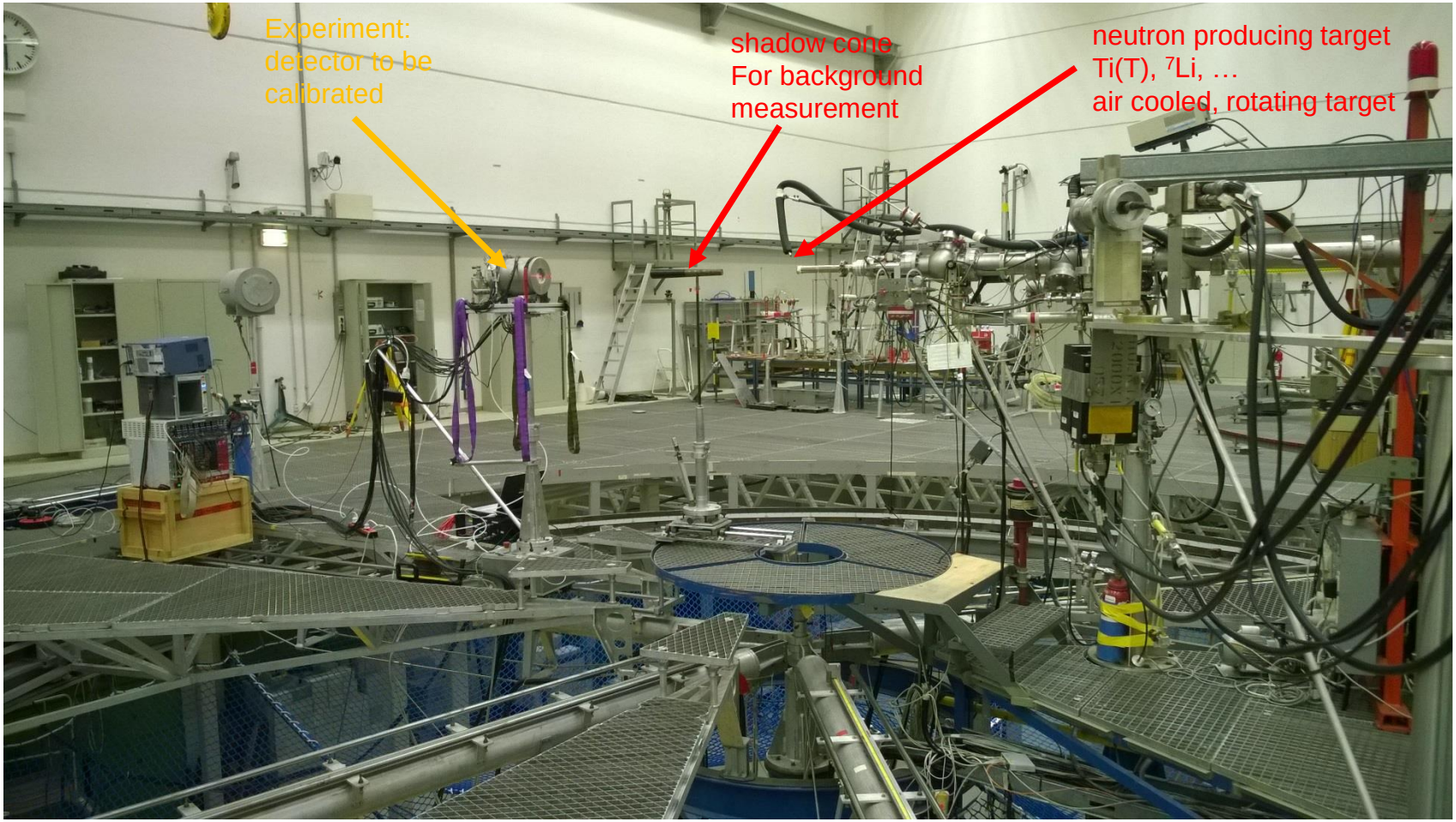

Neutron reference fields are produced in open geometry without collimation
Very low room return due to large free space around source and detectors
Van der Graaff Ion accelerator for 1 – 4 MeV protons, deuterons
with DC beam and pulsed beam Δt = 1-2ns, $\nu \approx 1$ MHz

Schematic time of flight measurement

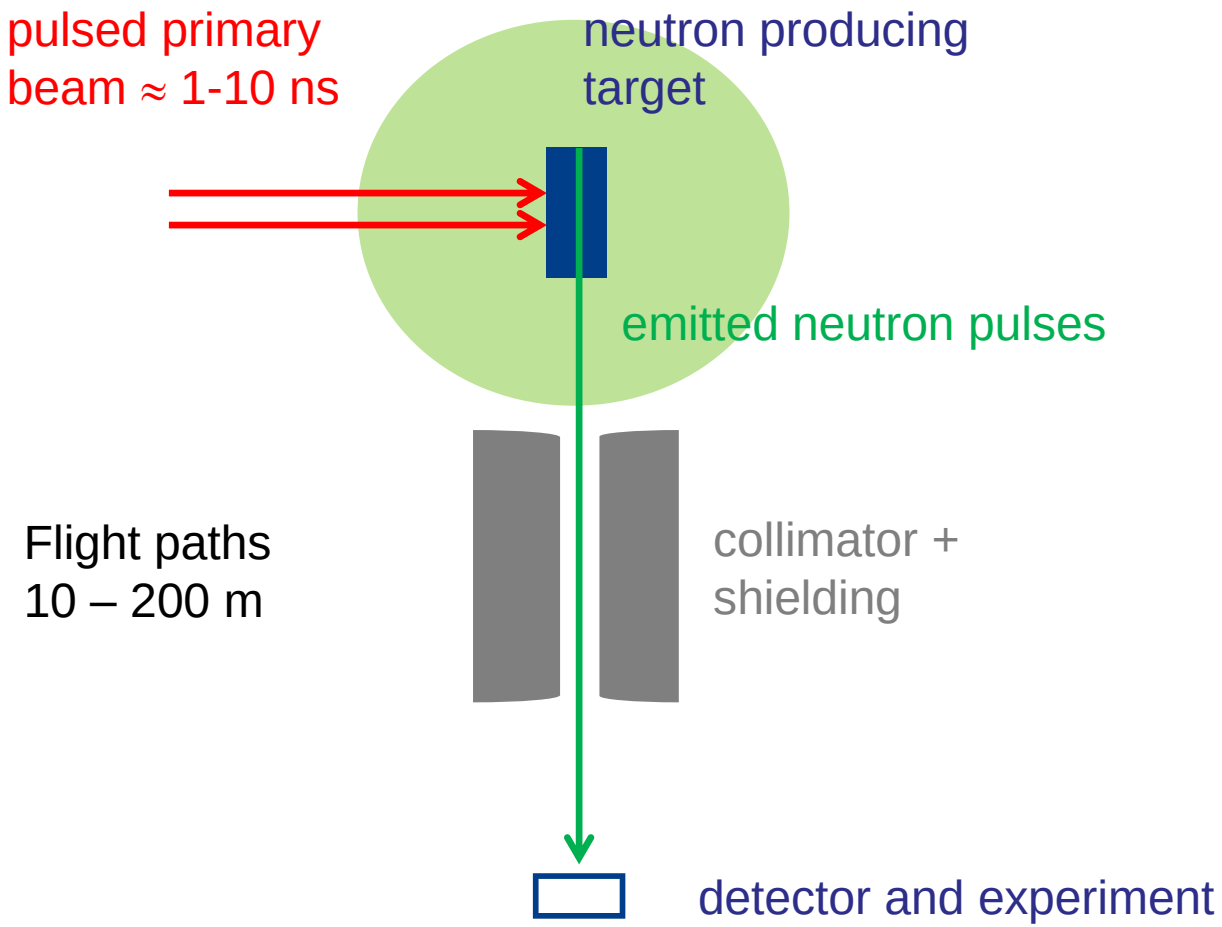

primary beams:

light charged particles with >100 MeV energy
➔ spallation neutron source

electrons 10 – 150 MeV
➔ photoneutron source

Deuteron beams on Be/C converters
deuteron break up

quasimonoenergetic neutron sources e.g. ^{7}Li(p,n)
➔ pulsed beam background identification

Energy resolved measurements by time of flight:

- Measurement of time-of-flight t and flight path l

1. $v = \frac{l}{t}$
2. $\gamma = \frac{1}{\sqrt{1-\left(\frac{v}{c}\right)^2}}$
3. $E = mc^2(\gamma - 1)$ *(E is the neutron kinetic energy)*

- Energy resolution

1. $\frac{\Delta E}{E} = (\gamma + 1)\gamma \frac{\Delta v}{v}$
2. $\frac{\Delta v}{v} = \sqrt{\left(\frac{\Delta t}{t}\right)^2 + \left(\frac{\Delta l}{l}\right)^2}$

- accelerator pulse length, time resolution of detectors, neutron transport in the neutron producing target and detector or sample Schillebeeckx et al. NDS 113 (2012) 3054

Time-of-flight to Energy correlation

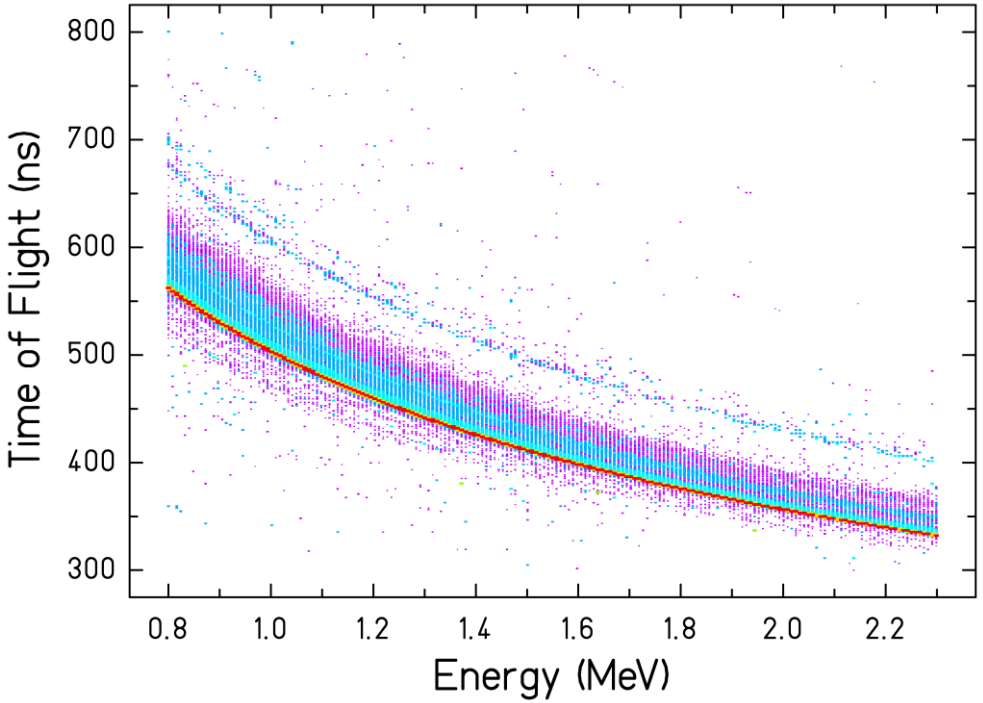

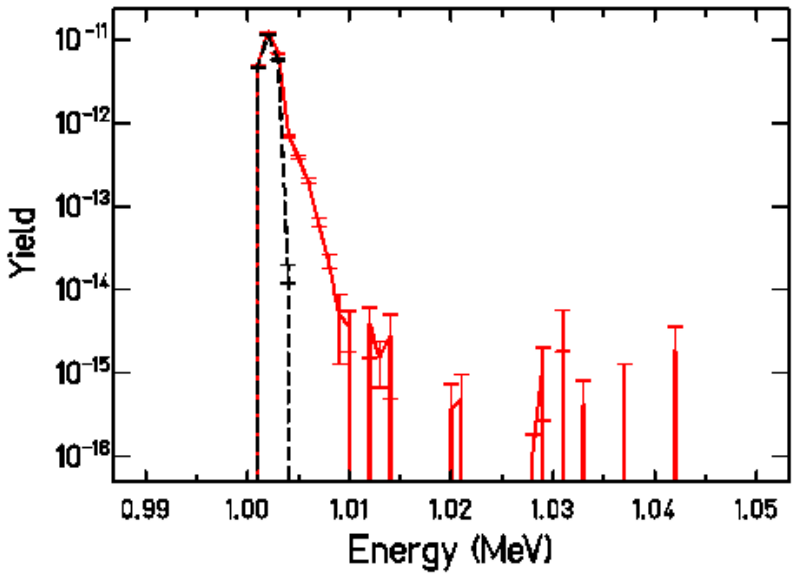

- Neutron transport code MCNP:
  Simulation of **neutron scattering** inside the neutron source and all surrounding materials e.g. collimators
- **Neutron scattering can change the correlation of time of flight and neutron energy ➔ multiple scattering corrections**

- Unscattered neutrons can be identified
  (in the simulation)

Neutron production by spallation

Relativistic protons impinging on heavy target nuclei

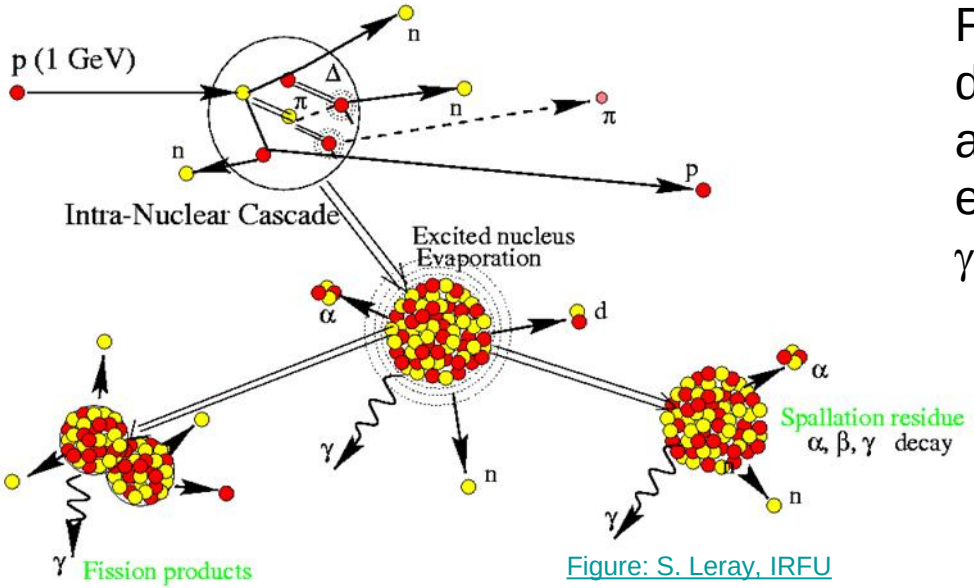

Figure: S. Leray, IRFU

Fast neutrons emitted during collision and afterwards from excited residual nuclei
γ-flash from pion decay

Nucleon-Nucleus collisions at relativistic energies
(de Broglie wavelength < mean free path)
in two phases:

$T_{coll} < 10^{-22}$s : Collisions of the projectile nucleon with nucleons in the target (Intranuclear Cascade, emission of **fast** particles π,**n**,p,…)

$T_{equil} > 10^{-21}$s – 10^{-16}s Reorganisation of the residual nuclei, thermalization, **particle evaporation** (**n**,p,d,α,…), gamma ray emission

Liège Intranuclear cascade model INCL
A. Boudard. Phys. Rev. C 87, 014606

Spallation neutron yield

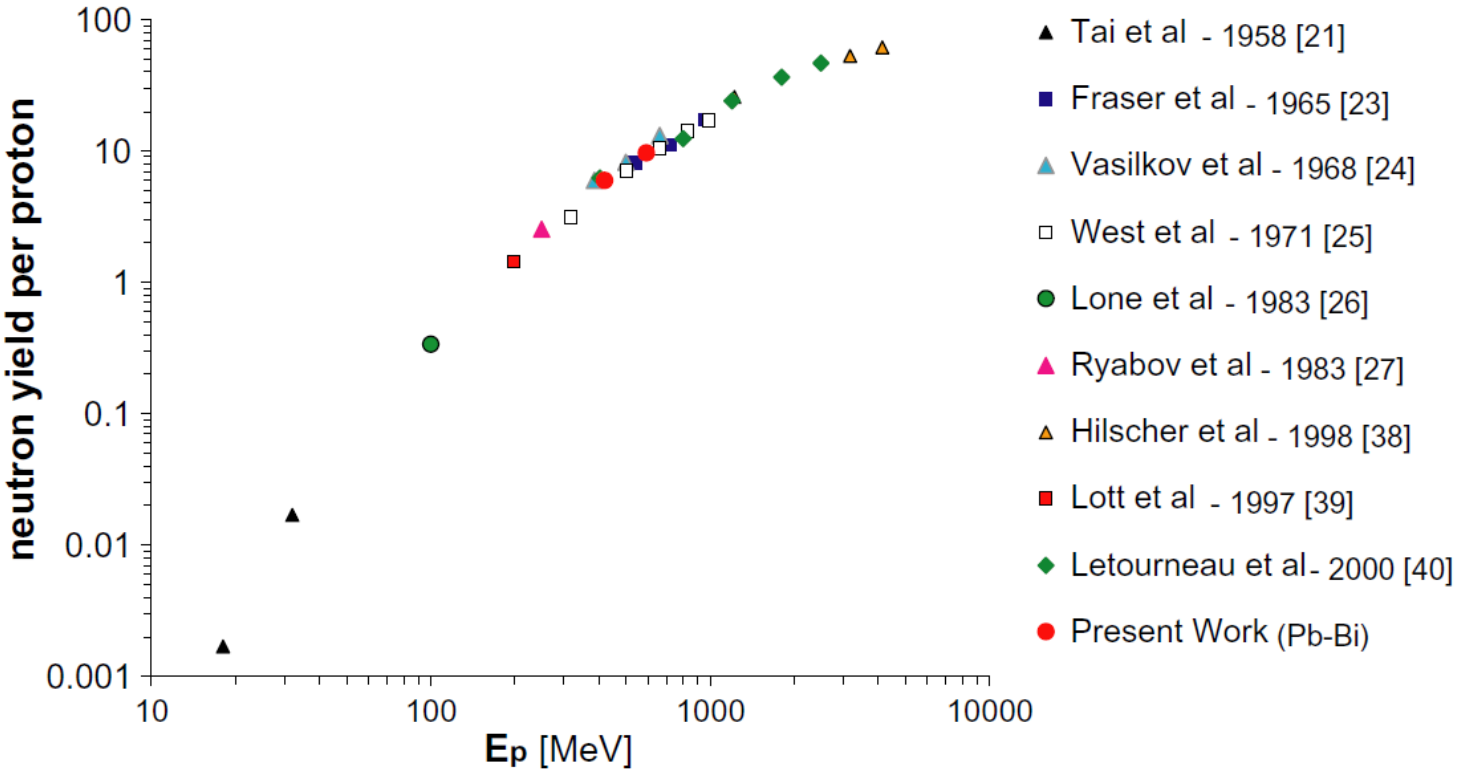

Fig. 10. Compilation of thick-target n/p values for p + Pb and Pb/Bi measured to date at all incident energies.

CERN nTOF ca. 300 n/p 20 GeV protons on Pb

K. Van der Meer, NIM B 217 (2004) 202–220

Neutron evaporation spectrum from Compound Nucleus decay

CN decay probability:

$$W_{c\beta}(\epsilon_\beta) = \frac{\rho_B(U)}{\rho_c(E)} \frac{m_\beta \epsilon_\beta \sigma_{\beta c}(\epsilon_\beta)}{\pi^2 \hbar^3}$$

$$\rho_c \propto \frac{1}{T} e^{E/kT}$$

$$\rho_B \propto \frac{1}{T} e^{U/kT} = \frac{1}{T} e^{(E-\epsilon-S_n)/kT}$$

$$\frac{\rho_B(U)}{\rho_c(E)} = const \cdot e^{-\epsilon/kT}$$

$$W(\epsilon_\beta) = const \cdot \sigma_{\beta c} \epsilon_\beta e^{-\epsilon/kT}$$

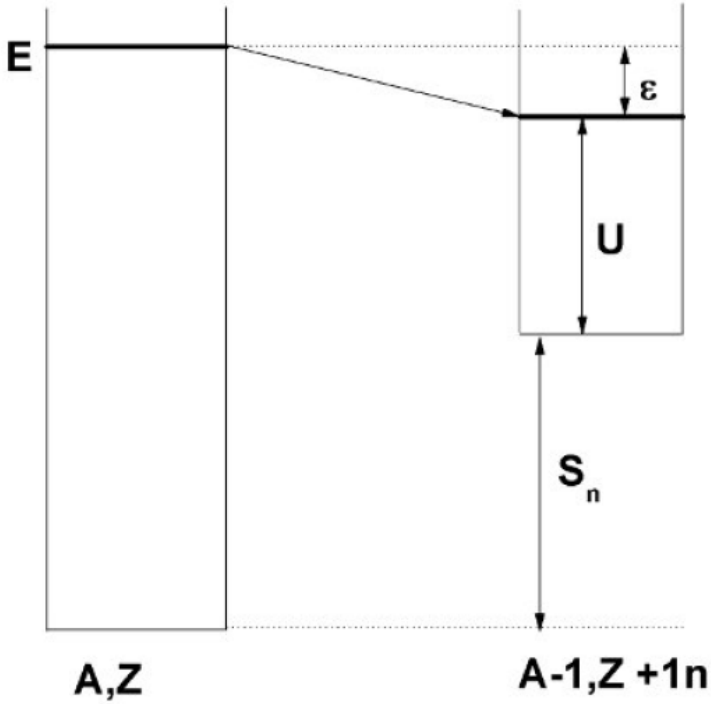

Compound nucleus c *Residual nucleus B*

$U = E - \varepsilon - S_n$

At ε close to max. transitions to discrete excited states of the residual nucleus B

The emission spectrum depends on:
The **level density** of the compound nucleus ρ_c
The **level density** of the residual nucleus ρ_B
and the inverse cross section of compound nucleus formation

For neutron emission $\sigma_{\beta c}$ is not strongly energy depend. ➔ Maxwellian energy spectrum
For charged particle emission: Transmission through the Coulomb-Barrier

Neutron evaporation spectra

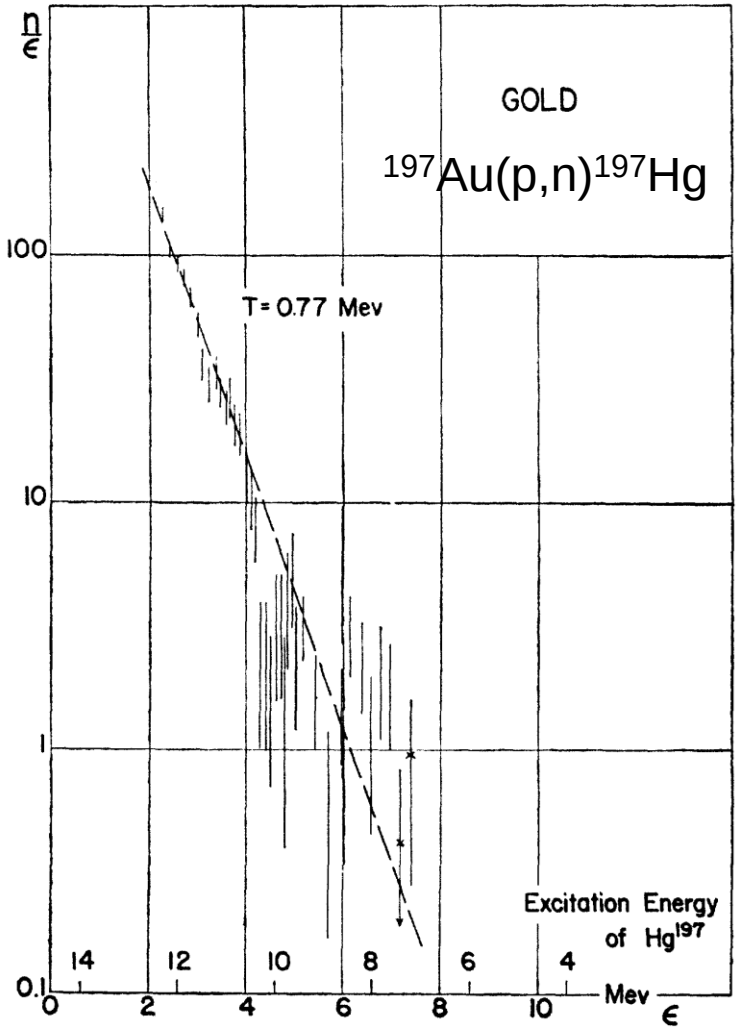

FIG. 11. Relative level density of Hg^{197}.

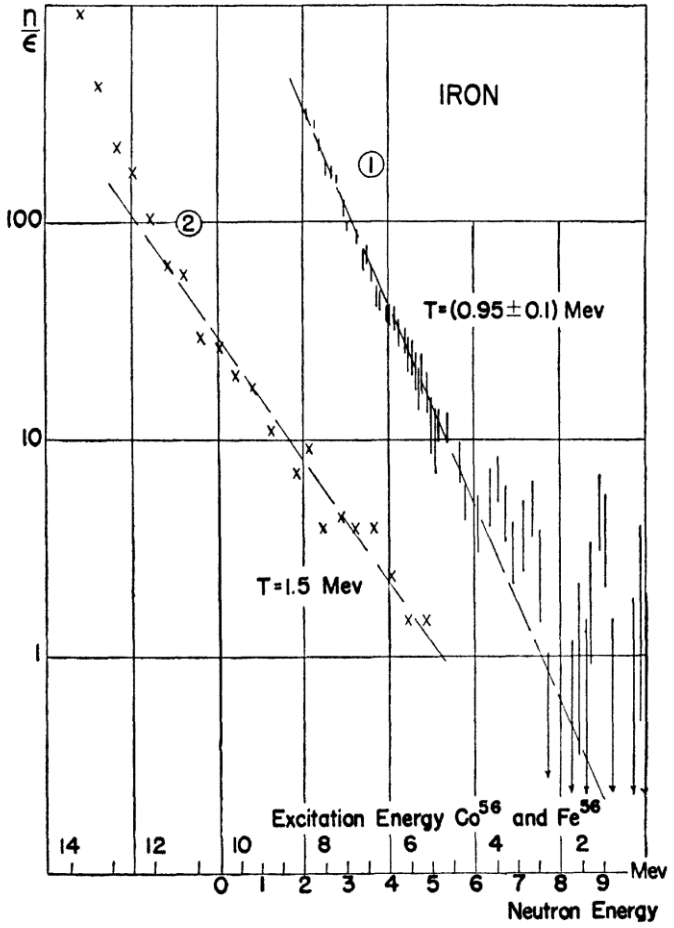

FIG. 9. Relative level density of Co^{56} and Fe^{56}. Curve 1: represents the relative level density for Co^{56} obtained from the neutron spectrum; curve 2: shows the relative level density of Fe^{56} as observed from the inelastic scattering of 16-Mev protons by iron (reference 38).

Gugelot, Phys. Rev. 81 (1951) 51

Photoproduction of neutrons with bremsstrahlung

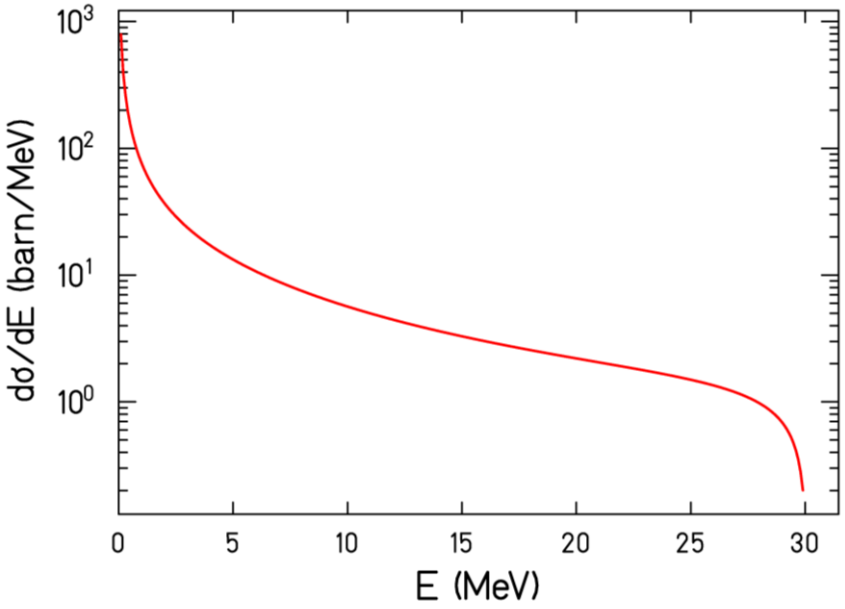

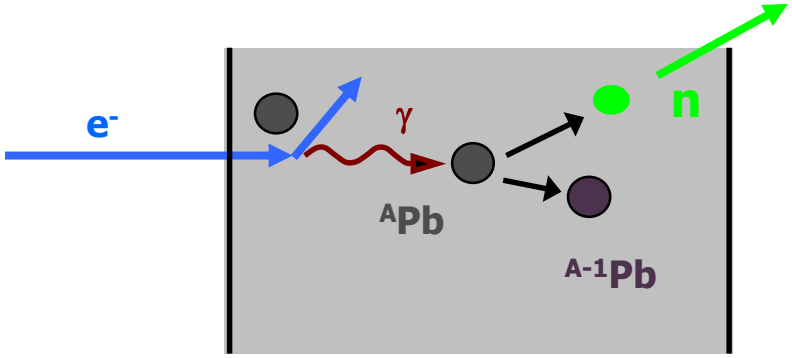

Bremsstrahlung spectrum ➔
Photonuclear excitation of Pb through the Giant Dipole Resonance (GDR)

Neutron production by
(γ,xn) reactions

nELBE yield: $3*10^{11}$ n/s with
30 MeV 15µA (Target:Pb,liquid)
200 kHz
GELINA yield: $3*10^{13}$ n/s with
100 MeV 96µA (Target: U(Hg cooled))
800 Hz

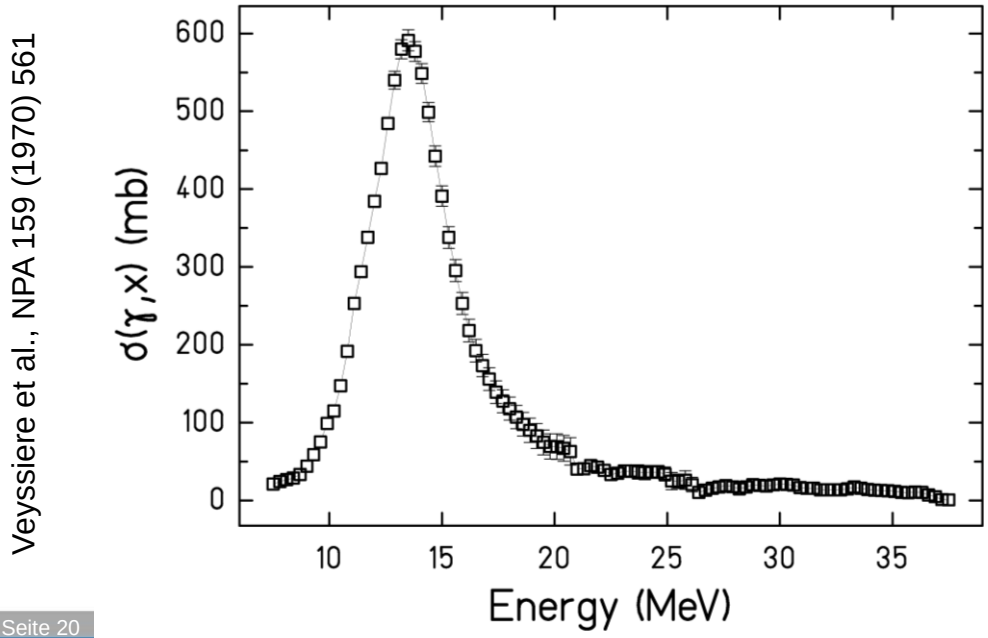

Veyssiere et al., NPA 159 (1970) 561

Photo neutron spectrum from nELBE

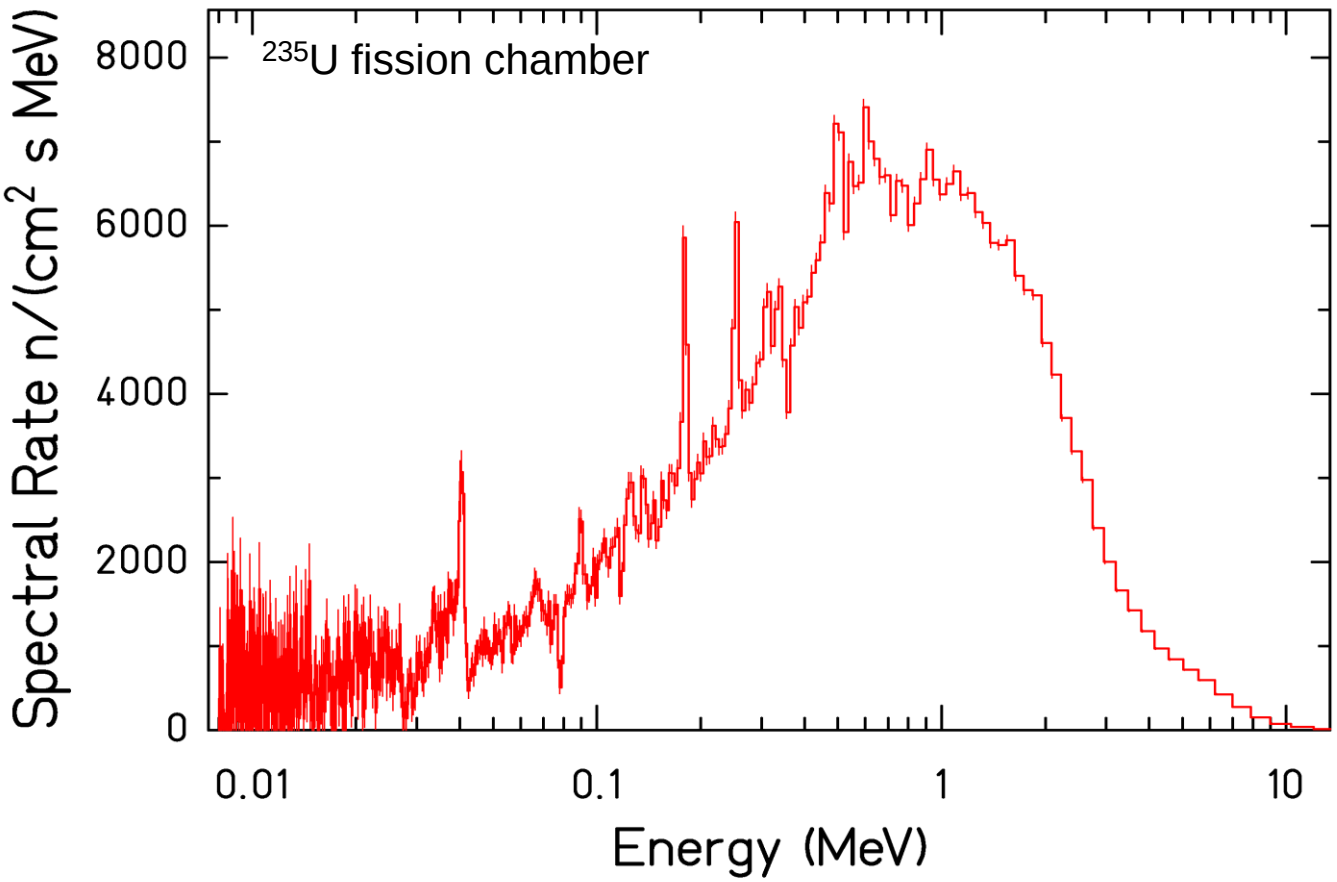

Measurement time : 49.4 h I_{e-} = 15 µA, E_{e-} = 31 MeV
Flight path 618 cm
Absorption dips : 78,117, 355, 528, 722, 820 keV ^{208}Pb scatttering resonances
Emission peaks: 40,89,179, 254, 314, 605 keV near threshold photoneutron emission
In ^{208}Pb (strong capture resonances of ^{207}Pb)

R. Beyer et al., NIM A723 (2013) 151

Prompt neutron production by fission

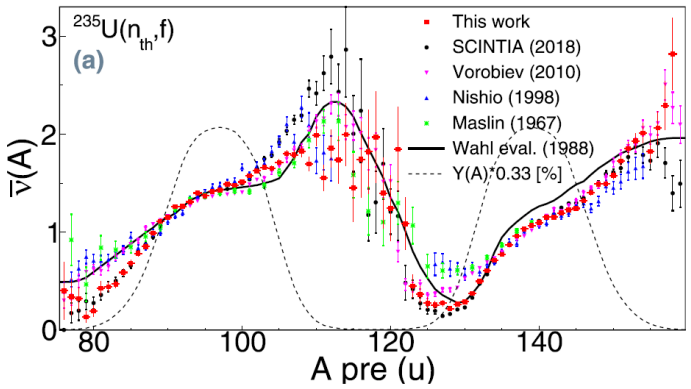

- Neutrons are mostly emitted from the accelerated fission fragments.
- Low energy fission shows saw-tooth behaviour of the average number of neutrons emitted from each fission fragment with mass number A

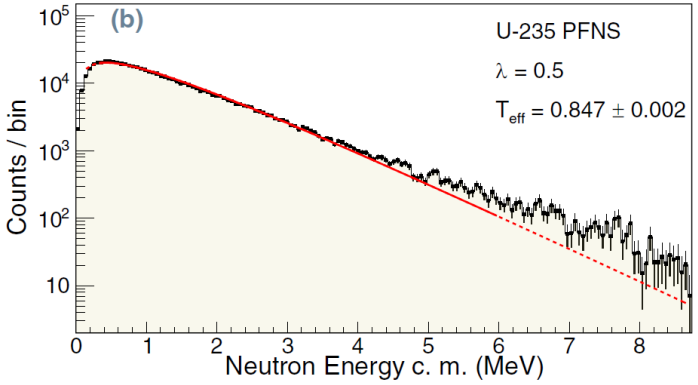

- Fission fragments are excited neutron-rich compound nuclei that deexcite by neutron and gamma-ray emission
- Neutron evaporation in statistical model

Van de Graaff accelerator, JRC Geel
TFGIC + liquid scintillators
A. Al-Adili, Phys. Rev. C102 (2020) 064610

e.g. Los Alamos Model for prompt fission neutrons
D.G. Madland, Nuclear Physics A 957 (2017) 289–311

Accelerator-based Neutron Sources

- **Time-of-flight neutron sources**
- High energy resolution for resolved resonance region:
  Gelina JRC Geel, nELBE HZDR Dresden, n_TOF CERN
- Quasimonoenergetic and 'white' beams < 40 MeV: **NFS Ganil**
- Dedicated detector systems for (n,n'γ) and (n,tot) measurements

NFS (GANIL), n_TOF lead target 3 (CERN) + NEAR station

- **Ion accelerators**
- Quasimonoenergetic and 'white' neutrons for unresolved resonance region
  - Electrostatic accelerators :
    CNRS-AIFIRA Bordeaux, CEA Bruyeres le Chatel, PTB Braunschweig, NPL London, CAN Sevilla, CNRS-ALTO Paris
  - Cyclotrons: **PTB , NPI Rez**
- 14 MeV generators for high intensities:
  ENEA Frascati, UU Uppsala, CNRS-GENESIS Grenoble
- Ion beams for surrogate method, ISOL and IBA: **UO Oslo, JYU Jyväskylä, IFIN Budapest**

HISPANoS D+d source CAN Sevilla, NESSA 14 MeV generator UU, TANJA 2 MV Tandetron PTB, MR-TOF mass separator JYU Jyväskyla

Research Reactors

- Thermal cross sections, fission neutron spectra, fundamental physics with neutrons
- Dedicated instruments: Penning traps, fission fragment and gamma spectrometers, cold neutron sources
- Ultracold, cold and thermal neutrons:
  MTA-EK Budapest, SCK CEN Mol, CVŘ, Řez
- High-flux reactor: **ILL Grenoble**
- Pulsed source: **JGU TRIGA Mainz**
- Instruments for nuclear data:
  Prompt Gamma Activation Analysis
  Neutron induced Prompt gamma-ray spectroscopy
  Fission product prompt gamma-ray spectrometer
  Fission Yield measurements
  Fission fragment spectrometer

Beam properties of the ARIEL facilities

summary of the ARIEL facilities available for TAA		accelerators																			research reactors				
		e⁻ beams		ion beams																					
		nELBE@HZDR	GELINA@JRC	MONNET@JRC	n_TOF@CERN	AIFIRA@CNRS	ALTO@CNRS	GENESIS@CNRS	NFS@GANIL	CEA-DAM	FNG@ENEA	PTB	FNG@NPI	HISPANOS@CNA	NESSA@UU	U. Oslo	NPL	IFIN-HH	JYU	IRSN	AGOR@UMCG	BRR@mtaEK	BR1@SCK·CEN	TRIGA@JGU	LR-0/LVR-15 @CVR	RHF@ILL
neutrons	cold (<25 meV)																					■		■		■
	thermal (‹E_n›=25 meV)		■	■										■			■			■		■	■	■	■	■
	epithermal (25 meV – 100 keV)		■		■	■	■			■				■			■			■		■	■	■	■	■
	fast (0.1-20 MeV)	■	■	■	■	■	■	■	■	■	■	■	■	■	■		■			■		■	■	■	■	■
	very fast (>20 MeV)				■				■				■													
	pulsed beam	■	■	■	■				■	■		■	■	■	■					■				■		
	time-of-flight	■	■	■	■				■	■		■	■	■						■						
charged particles						■	■									■		■			■					
radioactive beam							■												■							■

LOHENGRIN Fission Fragment Spectrometer

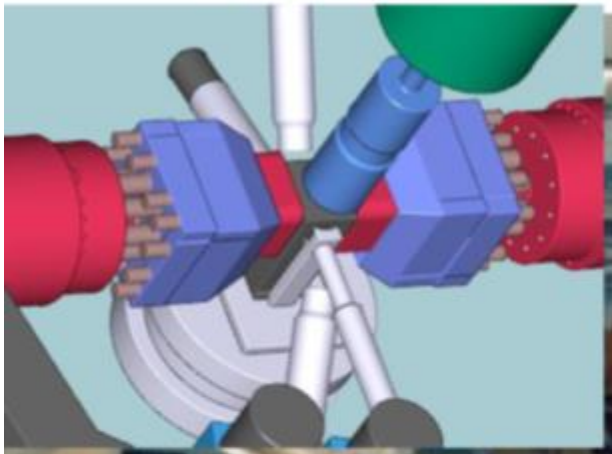

FF recoil spectrometer

$\frac{A}{\Delta A} \cong 400$; $\frac{E}{\Delta E} \cong 100$

-separation of ionic charge states ➔ fission yields

A. Chebboubi, Eur. Phys. J. A (2021) 57:335

PGAA's modular neutron flight tube applications

Removable modules enable to accommodate user supplied set up:

- Measurement of prompt fission gamma spectra of $^{233}U(n_{cold},\ f\ \gamma)$ with users from JRC Geel in 2018
- Fission chamber + gamma ray detectors (4 $LaBr_3$:Ce + HPGe)
- Relative (n, γ) Xsection measurement (^{242}Pu(n, γ) Univ. Sevilla, 2018)
- Isotopic analysis of samples (CERN, EFNUDAT)
- Gamma strength function (^{242}Pu(n, γ) Univ. Sevilla, 2018) and (^{232}Th(n, γ) Univ. Osmangazi, 2017, 2018)
- Gamma-gamma coincidence (^{94}Nb(n, $\gamma\gamma$), Univ. Novi Sad, 2016 and 2017)
- Etc.

CERN n_TOF Experiment

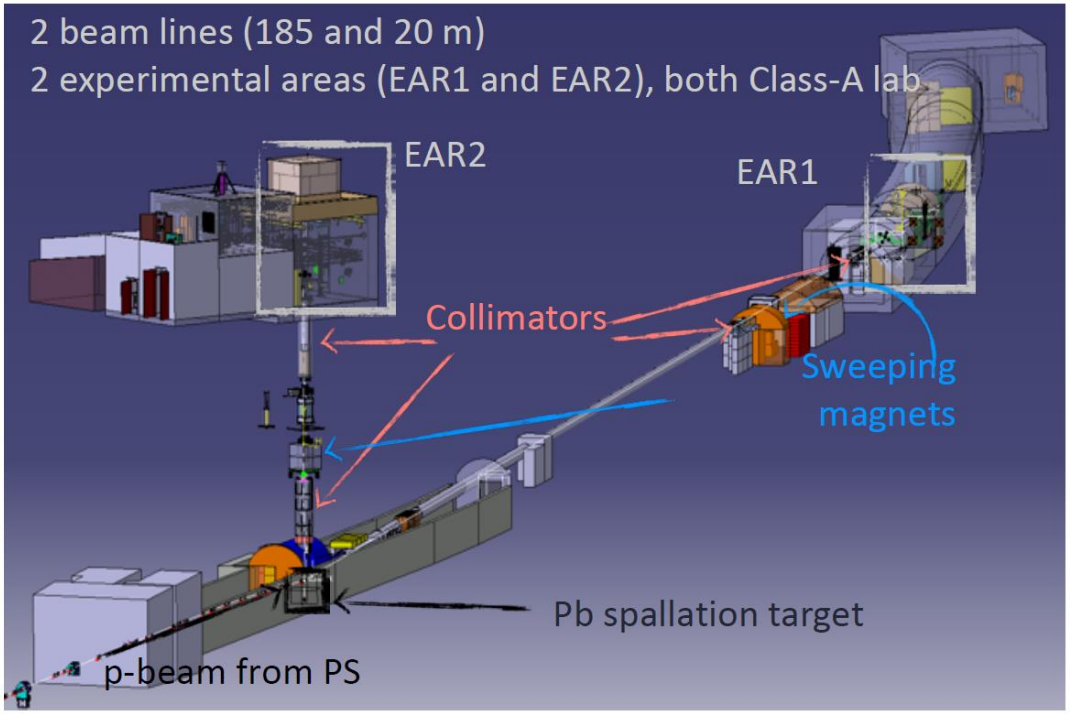

EAR-2:
short flight path 20 m for higher intensity
90° to the proton beam ➔ Background reduction

- Spallation source using 20 GeV/c proton beam from CERN proton synchrotron
- New spallation target in 2021 > 10^6 n / PS pulse
- Radioactive target capability at experimental stations (high instantaneous flux ➔ use of small number of target atoms)

Experimental capabilities:
radiative neutron capture (n,γ)
neutron induced fission (n,f)
Neutron induced light charged particle emission (n,p) (n,α)

NEAR station for irradiation

E.Chiaveri, EPJ Web of Conferences 239, 17001 (2020)

Spallation neutron spectrum at CERN nTOF

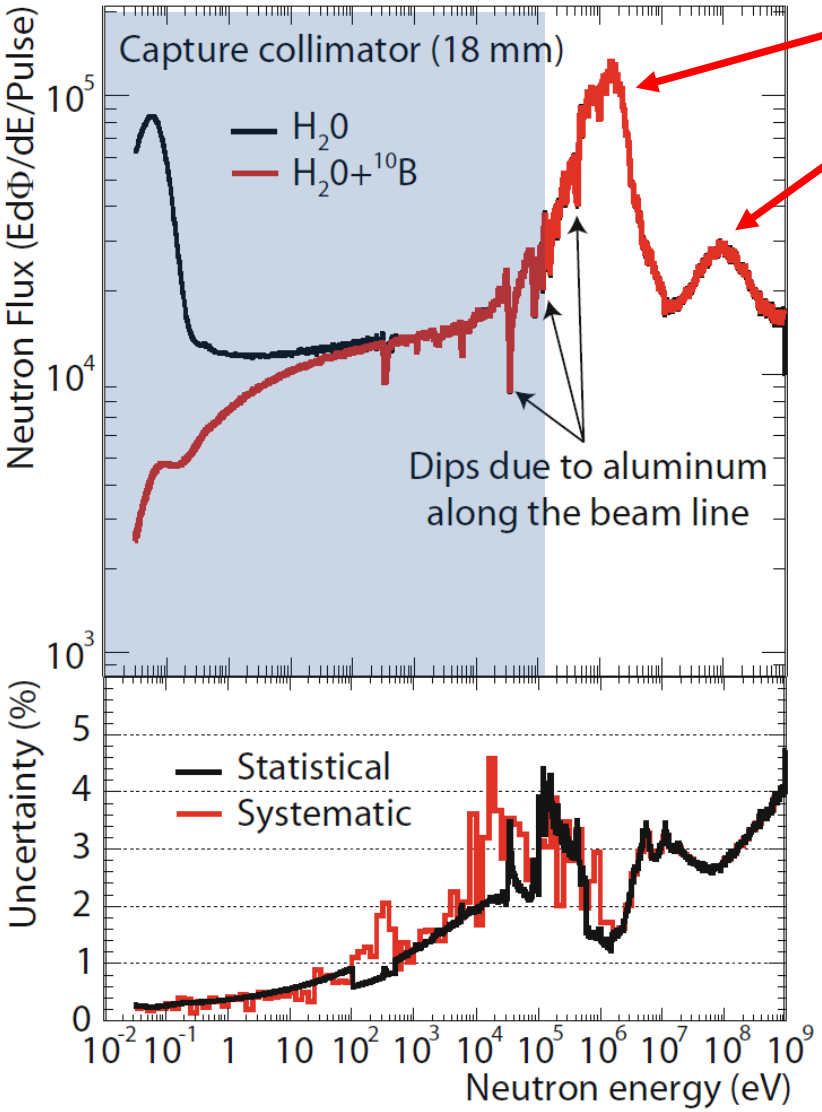

Neutron evaporation (0.1 – 10 MeV)

Fast neutrons from intranuclear cascade stage > 10 MeV

Shaded range < 0.1 MeV
Neutrons slowed down by hydrogeneous materials

ENERGY RESOLUTION

E_n (eV)	$\Delta E_n/E_n$
1	$4.3{\cdot}10^{-4}$
10	$4.3{\cdot}10^{-4}$
10^2	$4.3{\cdot}10^{-4}$
10^3	$7.5{\cdot}10^{-4}$
10^4	$1.7{\cdot}10^{-3}$
10^5	$5.4{\cdot}10^{-3}$
10^6	$2.8{\cdot}10^{-3}$

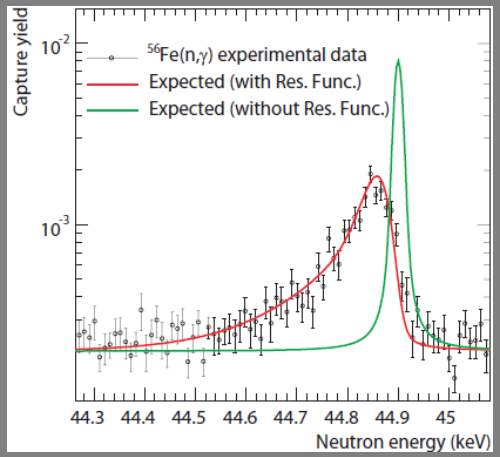

C. Guerrero et al., EPJA49 (2013) 27

GELINA pulsed neutron source

Electron accelerator

- 150 MeV electron accelerator
- 10 ns burst, 10 A peak
- 800 bursts/s

Compression magnet

- Pulse compression magnet
- <1 ns burst, >100 A peak

Electron-neutron conversion target

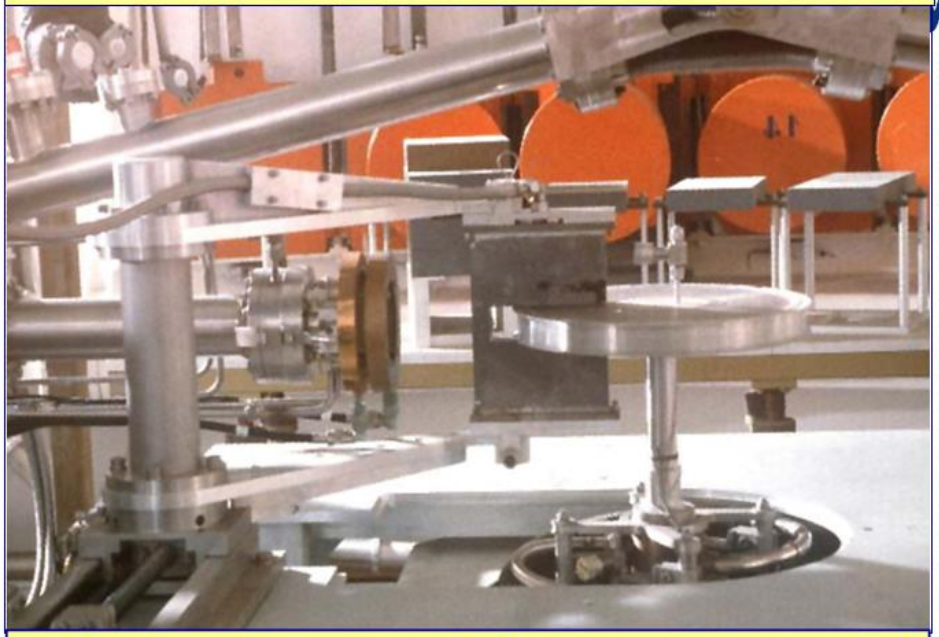

- Uranium target – rotating, mercury cooled
- 4 10^{10} neutrons / burst

water-filled Be moderators

12 Flight paths
8 to 400 m

moderated or fast neutron spectrum
24 h/d, 100 h/w

GELINA neutron spectrum and energy resolution

Flaska et al., NIM A531 (2004) 394

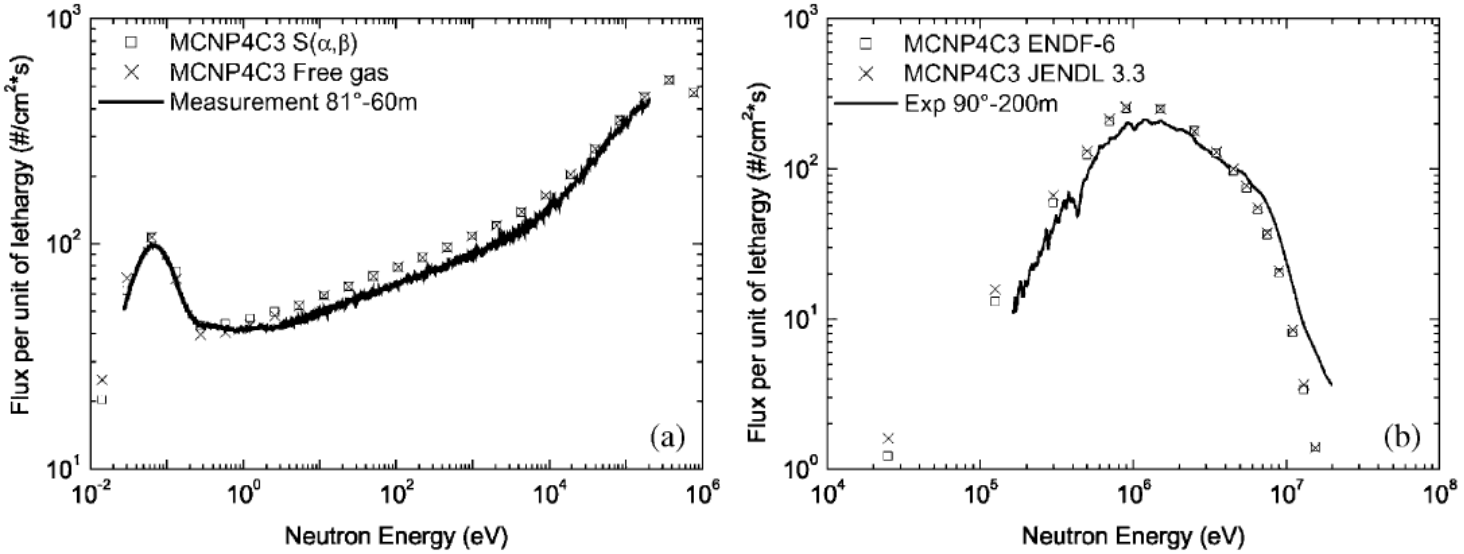

Fig. 4. Neutron flux per unit of lethargy in the flight-path. (a) 81°—60 m of the moderated neutron spectrum; (b) 90°—200 m of the fast neutron spectrum.

Schillebeeckx et al. NDS 113 (2012) 3054

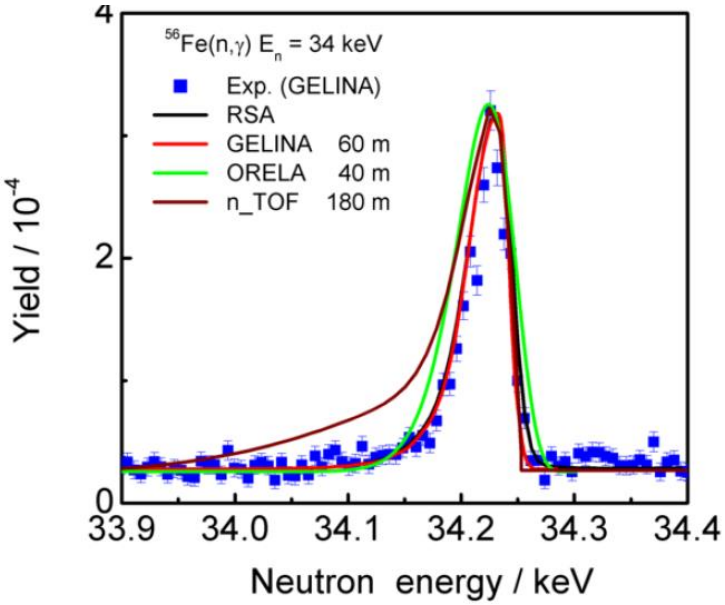

Fast neutron spectrum from 0.1 – 18 MeV

GELINA:

- width is dominated by the tof-resolution
  resonance total $\Gamma \approx 2$ eV
  Doppler width (FWHM) ≈ 13 eV
  ToF resolution (FWHM) ≈ 40 eV
- photoneutron sources tend to have a higher resolution than spallation neutron sources (larger target-moderators required)

Neutrons For Science at GANIL

- First facility at SPIRAL-2 superconducting LINAC
  proton (33 MeV), deuteron (40 MeV), helium (80 MeV) beams for neutron production
- F_0= 88 MHz with single bunch selector for ToF measurements 150 kHz – 1 MHz
  beam current 5 mA / N up to < 50 μA
- Thin and thick converter targets Li, C, Be
  quasimonoenergetic and continuous neutron spectra
- Irradiation station
- Radioactive target capability

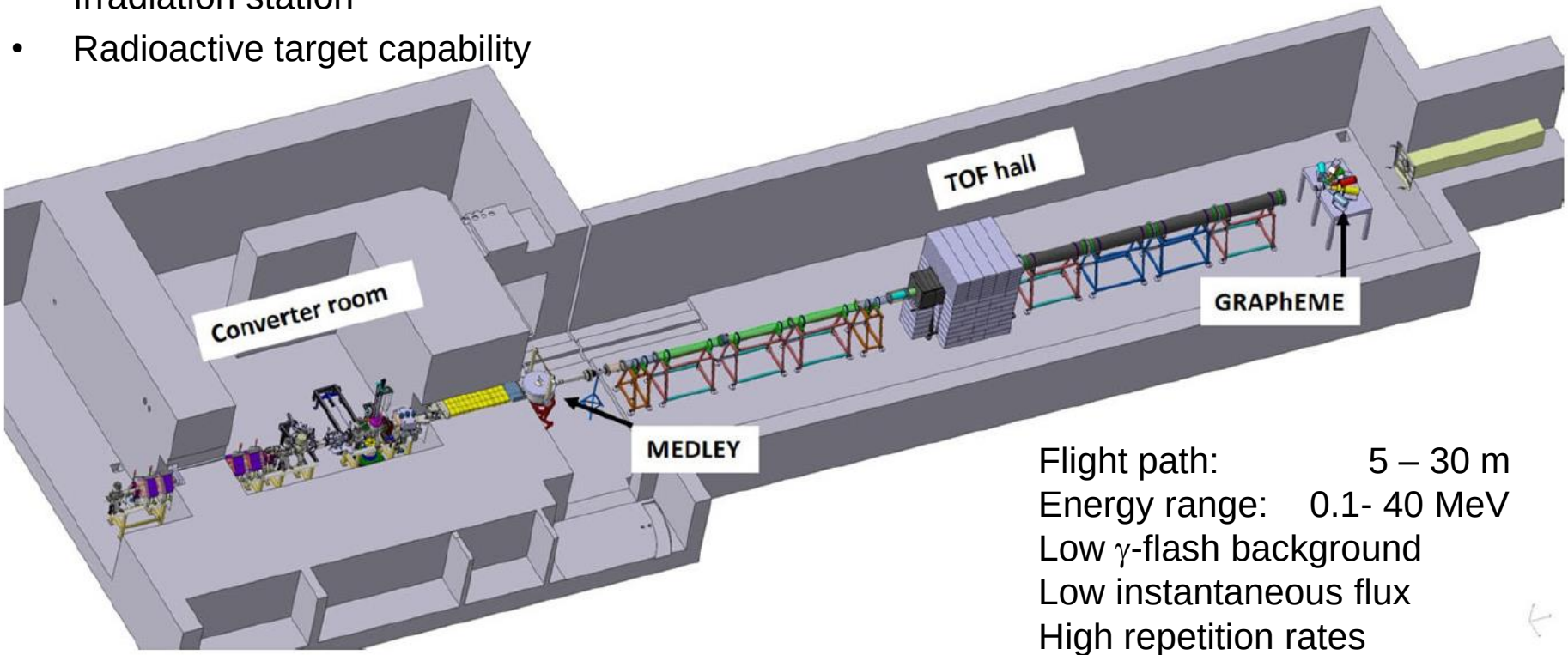

Flight path: 5 – 30 m
Energy range: 0.1- 40 MeV
Low γ-flash background
Low instantaneous flux
High repetition rates

X. Ledoux, Eur. Phys. J. A (2021) 57:257

NFS neutron spectra

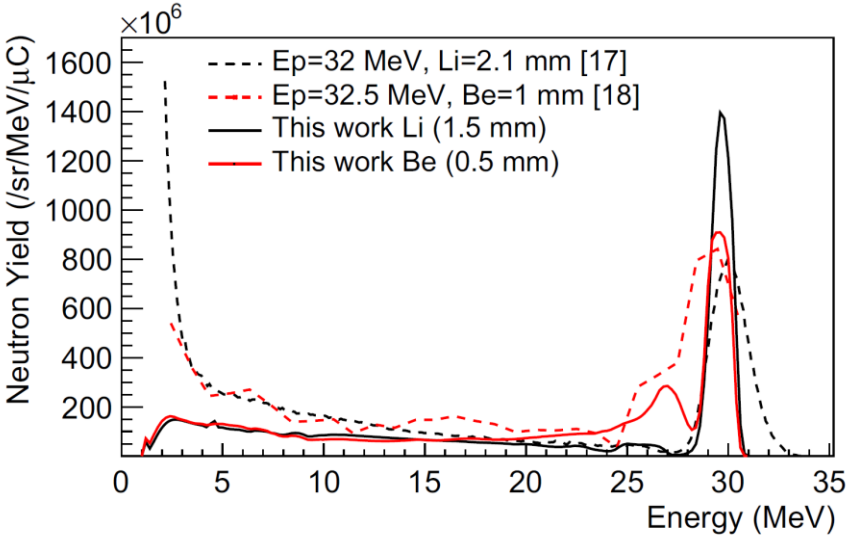

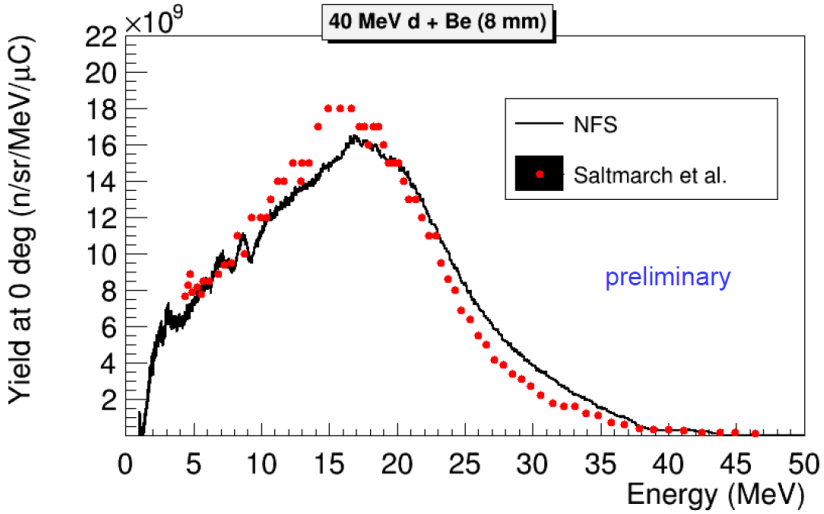

- Quasimonoenergetic neutrons
  p + ^{7}Li, ^{9}Be thin converters

- White spectrum 40 MeV deuterons on thick Be converter

Fast neutron range up to 40 MeV:
Reaction studies:
(n,n'γ),(n,xn), (n,f), (n,p), (n,α), (n,tot)

Flux at 5 meters : 8.10^{7} n/s/cm^2
at 15 MeV : 5.10^{6} n/s/cm^2/MeV
at 30 MeV : 6.10^{5} n/s/cm^2/MeV

X. Ledoux, Colloque Ganil 2021

Neutron time-of-flight facilities for cross section measurements

Facility	Type	particle energy (MeV)	Target	Pulse width (ns)	Frequency (Hz)	Flight Path Length (m)
GELINA	e-	80-140	U(Hg cooled)	1	40-800	10-400
nELBE	e-	40	Pb	0.01	100000-250000	4-10
NFS(GANIL)	d	40	Be,C	0.2	150000- 1000000	5-30
n_TOF (CERN)	p	20000	Pb	6	0.4	20,185
RPI	e-	60	Ta	7 - 5000	500	10-250
LANSCE - MLNSC	p	800	W	135	20	7-60
LANSCE -WNR	p	800	W	0.2	13900	8-90
JPARC/MLF - ANNRI	p	3000	Hg	600	25	21,28
CSNS back-n	p	1600	W(H2O cooled)	50 (double pulse)	25	55, 76
KURRI	e-	20-46	Ta	2,5,..100	1-300	10,13,24
KURRI	e-	7-32	Ta	100-4000	1-100	10,13,24
ORELA	e-	140	Ta	2 - 30	1-1000	10-200
POHANG	e-	75	Ta	2000	12	11

Literature

- Reference:
  J.B. Marion, J.L. Fowler, Fast Neutron Physics Part I+II, Interscience New York, 1960 (kinematics in chapter I.b)

- Quasimonoenergetic neutrons:
  R. Nolte, D.J. Thomas, Metrologia 48 (2011) S263

- Neutron sources and resonance parameter determination
  P. Schillebeeckx, Nuclear Data Sheets 113 (2012) 3054–3100

- ARIEL webpage with links to many neutron beam facilities

ENDE